Journal of Sound and Vibration (2001) **242**(2), 247–264
doi:10.1006/jsvi.2000.3353, available online at http://www.idealibrary.com on IDEAL®

NON-LINEAR DYNAMICS AND CHAOS CONTROL OF A PHYSICAL PENDULUM WITH VIBRATING AND ROTATING SUPPORT

Z.-M. Ge, C.-H. Yang, H.-H. Chen and S.-C. Lee

Department of Mechanical Engineering, National Chiao Tung University, Hsinchu, Taiwan, Republic of China

(*Received* 24 *June* 1999, *and in final form* 12 *July* 2000)

The dynamic behavior of a physical pendulum system of which the support is subjected to both rotation and vertical vibration are studied in this paper. Both analytical and computational results are employed to obtain the characteristics of the system. By using Lyapunov's direct method the conditions of stability of the relative equilibrium position can be determined. Melnikov's method is applied to identify the existence of chaotic motion. The incremental harmonic balance method is used to find the stable and unstable periodic solutions for the strong non-linear system. By applying various numerical results such as phase portrait, Pioncaré map, time history and power spectrum analysis, a variety of the periodic solutions and the phenomena of the chaotic motion can be presented. The effects of the changes of parameters in the system could be found in the bifurcation and parametric diagrams. Further, chaotic motion can be verified by using Lyapunov exponent and Lyapunov dimension. The global analysis of basin boundary and fractal structure are observed by the modified interpolated cell mapping method. Besides, non-feedback control, delayed feedback control, adaptive control, and variable structure control are used to control the chaos effectively.

1. INTRODUCTION

In the dynamics of a rigid body with a fixed point, the mechanics in question has three degrees of freedom. In engineering system, however, one often encounters rigid bodies attached to a base by a two-degree-of-freedom joint, consisting of a vertical axis and a horizontal one, which are mutually perpendicular. If a vertical rotation is given, the degree of freedom becomes one, yet the set of kinematically possible motions is still quite rich. The motion of such a physical pendulum with rotation and vibration of support will be considered in this paper, when there are no applied forces other than the gravity force [1, 2].

Most of the physical systems are non-linear in nature, and can be described by the non-linear equations of motion. Hence, the researches of non-linear systems are spreading quickly today. In the analysis of a non-linear dissipative system, first one usually tries to locate all the possible equilibrium positions and periodic solutions of the system, and to determine the stability of these solutions. Second, one observes how these solutions evolve as the system parameters are varied, which leads to different forms of bifurcation. A further work is to find the basins of attraction in the state space for each attractor, and also to see how the basins of attraction change with the system parameters. Through extensive

0022-460X/01/170247 + 18 $35.00/0

analytical investigations, analogue and numerical simulations, as well as experimental observations, it has been shown that a pendulum exhibits a rich variety of non-linear bifurcational phenomena [3–8]. In particular, much work has been done on how point equilibria, periodic and chaotic attractors are created, changed or destroyed as system parameters are varied. The mechanisms include the well-known local bifurcation, together with subharmonic cascades, intermittencies, crises, etc. The geometry of the basins and their boundaries can often play an important role in the sensitivity of attractors to, say, noise-induced intermittency [8].

The analytical analyses for this non-linear dynamical system are obtained by Lyapunov's direct method [9–11], the incremental harmonic balance method [12–16], and Melnikov's method [17]. Only some special approaches can be used to reveal some important dynamical characteristics of the non-linear system. Lyapunov's direct method is applied to obtain the conditions of stability of the relative equilibrium position. Here an undamping-free oscillation system is employed. The incremental harmonic balance method (IHB) is used to find the stable and unstable periodic solutions for the strong non-linear system. Further, Melnikov's method is used to measure the distance between unstable and stable manifolds when the external disturbance is small.

A number of numerical results such as phase portraits, Poincaré maps, power spectrum analysis, bifurcation diagrams, and Lyapunov exponents [18], and the modified interpolated cell mapping method [19] are used to study the dynamical behavior of the physical pendulum system. The phase portrait is a collection of trajectories that represent the solutions of these differential equations of motion in the phase space. A more informative representation of the periodic solutions is the Poincaré map method. The bifurcation is the special phenomenon in a non-linear system. As the parameters are changed in the non-linear dynamical system, the characteristics of the equilibrium points change as well. Chaotic motion is the motion that has a sensitive dependence on initial conditions in deterministic non-linear physical systems. The Lyapunov exponent test is a powerful method to measure the sensitivity of the dynamical system to changes in initial conditions. A new effective method, the modified interpolated cell mapping [19, 20], is used to obtain the global analysis of dynamic behavior of the non-linear system. The different initial conditions in different basins of attraction may lead to the different attractors. The fractal basin boundary is also obtained by this technique.

Various methods for control of chaos are presented. In practice, it is often desired that chaos can be avoided and that the system performance will be improved or changed in some way. Clearly, the ability to control chaos, that is to convert chaotic oscillations into desired regular ones with a periodic time dependence, would be beneficial in working with a particular system. For this purpose, non-feedback control, delayed feedback control, adaptive control, and variable structure control are used to control chaos. As a result, the chaotic system can be controlled effectively.

2. EQUATION OF MOTION

A physical pendulum has a rotating and vibrating support with mutually perpendicular axes (Figure 1). The motion will be described in terms of two Cartestian co-ordinates, inertial system $OX_1X_2X_3$ and a moving co-ordinate system $ox_1x_2x_3$ rigidly attached to the physical pendulum. The origin of both co-ordinate systems is the point of intersection O of the joint axis; X_3- and x_1-axis are the fixed and moving axes of the joint respectively. All the kinematical possibility of the body relative to the inertial system $OX_1X_2X_3$ can be described in terms of two angles: the angle α between the X_1- and x_1-axis, and the angle

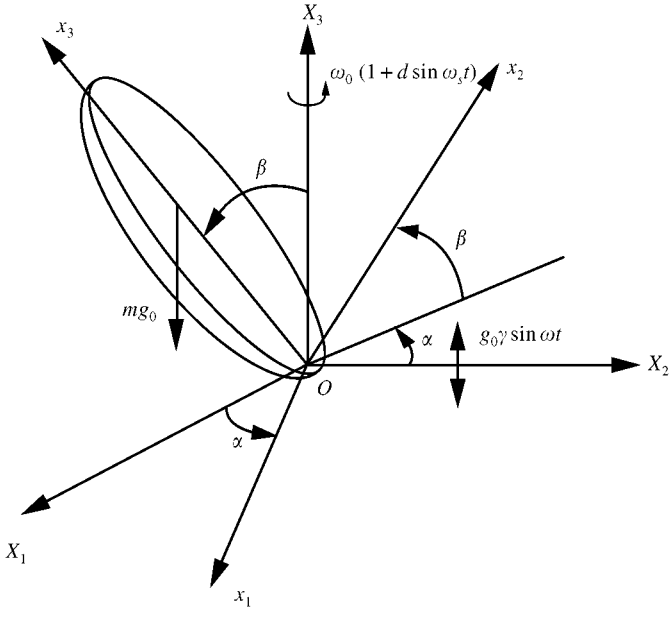

Figure 1. A schematic diagram of the physical pendulum.

β between the x_2 and X_1X_2 plane. The angles α and β, which will be taken as generalized co-ordinates, may be treated as the angles of two successive rotations through which one can transfer the rigid body from its initial position ($\alpha = \beta = 0$, the moving co-ordinate system coincides with the fixed one) to the present position.

Let ω_i denote the projection of the angular velocity vector ω of the body onto the x_i ($i = 1, 2, 3$)-axis. The kinematic equations expressing the components ω_i by α, β, $\dot{\alpha}$ and $\dot{\beta}$ are

$$\omega_1 = \dot{\beta}, \quad \omega_2 = \dot{\alpha}\sin\beta, \quad \omega_3 = \dot{\alpha}\cos\beta, \tag{2.1}$$

where $\dot{\alpha}$, $\dot{\beta}$ re generalized velocities. The kinetic energy of the motion of a rigid body with a fixed point is

$$T = \tfrac{1}{2}\,\{\varpi\}^{\mathrm{T}}\,\|J\|\,\{\varpi\}, \tag{2.2}$$

where $\|J\|$ is the inertia tensor of the body relative to the fixed point and $\{\varpi\}^{\mathrm{T}} = \{\omega_1, \omega_2, \omega_3\}$.

Expanding the scalar product in equation (2.2) taking equation (2.1) into account, we obtain

$$KE = \tfrac{1}{2}K(\beta)\dot{\alpha}^2 + \tfrac{1}{2}J_{11}\dot{\beta}^2 - b(\beta)\dot{\alpha}\dot{\beta}, \tag{2.3}$$

$$K(\beta) = J_{22}\sin^2\beta + J_{33}\cos^2\beta - 2J_{23}\sin\beta\cos\beta,$$

$$b(\beta) = J_{12}\sin\beta + J_{13}\cos\beta,$$

where J_{ii} ($i = 1, 2, 3$) are the axial moments of inertia and $J_{ij} = J_{ji}$ ($i \neq j, i, j = 1, 2, 3$) are the products of inertia of the body in $Ox_1x_2x_3$ co-ordinate system.

The inertial system $OX_1X_2X_3$ is now appointed to a vertical vibration with acceleration $\mathbf{g}_0\ \gamma\sin\omega t$ where $\mathbf{g}_0$ is gravitational acceleration, $0 < \gamma < 1$ is constant, ω is the given frequency of the vibration of support. The potential energy of the motion of the physical

pendulum in non-inertia system $OX_1X_2X_3$ is

$$PE = mg_0h(1 + \gamma \sin \omega t)\cos\beta, \tag{2.4}$$

where m is the mass of pendulum and h is the distance of center of mass to fixed point. By Lagrangian approach the Lagrangian has the expression

$$L = \tfrac{1}{2}K(\beta)\dot{\alpha}^2 + \tfrac{1}{2}J_{11}\dot{\beta}^2 - b(\beta)\dot{\alpha}\dot{\beta} - mg_0h(1 + y\sin\omega t)\cos\beta. \tag{2.5}$$

When angular velocity $\dot{\alpha} = \omega_0(1 + d\sin\omega_s t)$ is given to the vertical rotation, the degree of freedom of the system is reduced to one, where ω_0, $0 < d < 1$, and ω_d are constants. The Lagrange equation corresponding to equation (2.5) is

$$J_{11}\ddot{\beta} - (\omega_0\omega_s d\cos\omega_s t)b(\beta) - \tfrac{1}{2}Z(\beta)\dot{\alpha}^2 + C\dot{\beta} - mg_0h(1 + \gamma\sin\omega t)\sin\beta = 0. \tag{2.6}$$

where

$$Z(\beta) = (J_{22} - J_{33})\sin 2\beta - 2J_{23}\cos 2\beta$$

and C is the coefficient of damping.

Changing the time scale $\tau = \omega_n t$, equation (2.6) can be written in dimensionless form. Define

$$\omega_n^2 = \frac{mg_0h}{J_{11}}$$

If $\omega_s = \omega$ then equation (2.6) becomes

$$\ddot{\beta} - (\rho\eta d\cos\eta\tau)\bar{b}(\beta) - \tfrac{1}{2}\bar{Z}(\beta)\dot{\alpha}_1^2 + \bar{C}\dot{\beta} - (1 + \gamma\sin\eta\tau)\sin\beta = 0, \tag{2.7}$$

where

$$\rho = \frac{\omega_0}{\omega_n}, \quad \eta = \frac{\omega}{\omega_n}, \quad \bar{b}(\beta) = \frac{b(\beta)}{J_{11}}, \quad \bar{Z}(\beta) = \frac{Z(\beta)}{J_{11}}, \quad \bar{C} = \frac{C}{J_{11}\omega_n},$$

$$\tau = \omega_n t, \quad \dot{\alpha}_1 = \varepsilon(1 + d\sin\eta\tau).$$

If $\omega_s \neq \omega$ equation (2.6) becomes

$$\ddot{\beta} - (\rho\eta_s d\cos\eta_s\tau)\bar{b}(\beta) - \tfrac{1}{2}\bar{Z}(\beta)\dot{\alpha}_1^2 + \bar{C}\dot{\beta} - (1 + \gamma\sin\eta\tau)\sin\beta = 0, \tag{2.8}$$

where

$$\eta_s = \frac{\omega_s}{\omega_n}.$$

3. STABILITY ANALYSIS BY LYAPUNOV DIRECT METHOD

In this section, the stabilities of steady motion of the autonomous system are studied, where $\dot{\alpha} = \omega_0 = const$, $\gamma = 0$, $C = 0$ and J_{23} is assumed to be zero. The kinetic energy for this system is

$$T = \tfrac{1}{2}(J_{22}\sin^2\beta + J_{33}\cos^2\beta)\omega_0^2 + \tfrac{1}{2}J_{11}\dot{\beta}^2 - (J_{12}\sin\beta + J_{13}\cos\beta)\omega_0\dot{\beta}, \tag{3.1}$$

The potential energy Π is

$$\Pi = mg_0h\cos\beta. \tag{3.2}$$

The Lagrangian of the system becomes

$$L = T - \Pi = \tfrac{1}{2}(J_{22}\sin^2\beta + J_{33}\cos^2\beta)\omega_0^2 + \tfrac{1}{2}J_{11}\dot{\beta}^2 - (J_{12}\sin\beta + J_{13}\cos\beta)\omega_0\dot{\beta} - mg_0h\cos\beta. \tag{3.3}$$

The Lagrange differential equation of motion is

$$\frac{\mathrm{d}}{\mathrm{d}t}\left(\frac{\partial L}{\partial \dot{\beta}}\right) - \frac{\partial L}{\partial \beta} = 0 \tag{3.4}$$

which is presented as

$$J_{11}\ddot{\beta} - \tfrac{1}{2}Z(\beta)\omega_0^2 - mg_0h\sin\beta = 0, \tag{3.5}$$

where

$$Z(\beta) = (J_{22} - J_{33})\sin 2\beta. \tag{3.6}$$

Expanding $\sin\beta$ and $\cos\beta$ as power series, it can be written as

$$\dot{\beta}_1 = \beta_2,$$

$$\dot{\beta} = \frac{1}{J_{11}}[(J_{22} - J_{33})\omega_0^2 + mg_0h]\beta_1 + \cdots, \tag{3.7}$$

where $\beta_1 = \beta$, $\beta_2 = \beta$, and the higher order terms are neither presented nor neglected.

The stability of steady motion $\beta = 0$ is studied. Since the Lagrangian of the system does not contain t explicitly, there exists the Jacobi integral [2]

$$T_2 - T_0 + \Pi = \text{const.},$$

where T_2 denotes the quadratic terms of $\dot{\beta}$ in kinetic energy and T_0 the terms free from $\dot{\beta}$ in kinetic energy.

The Jacobi integral is chosen as the Lyapunov function

$$V = T_2 - T_0 + \Pi = \tfrac{1}{2}[(J_{33} - J_{22})\omega_0^2 - mg_0h]\beta_1^2 + \tfrac{1}{2}J_{11}\dot{\beta}_2^2 + \cdots. \tag{3.8}$$

If

$$(J_{33} - J_{22})\omega_0^2 - mg_0h > 0, \tag{3.9}$$

$\bar{V}$ is positive definite for all higher order terms [9]. Since V is a first integral,

$$\frac{\mathrm{d}V}{\mathrm{d}t} = 0. \tag{3.10}$$

By Lyapunov's stability theorem, the steady motion is stable [9].

For the study of instability, the Lyapunov function is chosen as

$$V = \beta_1\beta_2. \tag{3.11}$$

The time derivative of V through equation (3.7) becomes

$$\dot{V} = [mg_0h - (J_{33} - J_{22})\omega_0^2]\beta_1^2 + \beta_2^2 + \cdots \tag{3.12}$$

If

$$(J_{33} - J_{22})\omega_0^2 - mg_0h < 0, \tag{3.13}$$

$\dot{V}$ is positive definite for all higher order terms. By Lyapunov's instability theorem [9] equation (3.13) is the condition of instability.

4. INCREMENTAL HARMONIC BALANCE METHOD

The IHB method is a combination of the incremental method with the harmonic balance method. The steady state periodic solutions of equation (2.6) are obtained by the IHB method, which can deal very well with strong non-linearity and is convenient for computer implementation [12–16].

From equation (2.6), let $\tau_1 = \omega t$, $\omega_0 = \omega$, the dimensionless equation is given as

$$\omega^2 \beta'' - (\omega_0 \omega d \cos\tau_1)\bar{b}(\beta) - \tfrac{1}{2}\bar{Z}(\beta)\dot{\alpha}^2 + c_1 \omega \dot{\beta} - v_1(1 + \gamma \sin\tau_1)\sin\beta = 0, \tag{4.1}$$

where

$$\beta' = \frac{\mathrm{d}\beta}{\mathrm{d}\tau_1}, \quad c_1 = \frac{C}{J_{11}}, \quad v_1 = \frac{mg_0 . h}{J_{11}}$$

The first step of the IHB method is a Newton–Raphson procedure. Let β_0, ω_{00}, ω_{10} and γ_0 be solutions; the neighboring state can be expressed by adding the corresponding increments to them as follows:

$$\beta = \beta_0 + \Delta\beta, \quad \omega = \omega_{00} + \Delta\omega, \quad \omega_0 = \omega_{10} + \Delta\omega_1, \quad \gamma = \gamma_0 + \Delta\gamma. \tag{4.2}$$

Substituting equation (4.2) into equation (4.1) and neglecting the small terms of higher order, the linearized incremental equation can be derived as

$$\omega_{00}^2 \beta'' + c_1 \omega_{00} \beta' + \Delta\beta g_1(\beta_0, \tau_1) = R + \Delta\omega S + \Delta\omega_1 E + \Delta\gamma P, \tag{4.3}$$

where

$$g_1(\beta_0, \tau_1) = \omega_{10}\omega_{00}\bar{b}' d \cos\tau_l + \tfrac{1}{2}\dot{\alpha}^2 \bar{Z}' + (1 + \gamma_0 \sin\tau_l)\cos\beta_0,$$

$$R = -(\omega_{00}^2 \beta'' + c_1 \omega_{00} \beta' + g_2(\beta_0, \tau_1)),$$

$$g_2(\beta_0, \tau_1) = \omega_{10}\omega_{00}\bar{b} d \cos\tau_1 + \tfrac{1}{2}\dot{\alpha}^2 \bar{Z} + (1 + \gamma_0 \sin\tau_1)\sin\beta_0,$$

$$S = -(2\omega_0 \beta'' + c_1 \beta' - \omega_{10}\bar{b} d \cos\tau_1),$$

$$E = \omega_{00}\bar{b} d \cos\tau_1 + \omega_{10}\dot{\alpha}^2 \bar{Z}, \; P = -\sin\tau_1 \sin\beta_0,$$

$$\bar{b} = \frac{J_{12}\cos\beta_0 - J_{13}\sin\beta_0}{J_{11}},$$

$$\bar{Z}' = \frac{2((J_{22} - J_{33})\cos 2\beta_0 + 2J_{23}\sin 2\beta_0)}{J_{11}}$$

and R is a corrective vector which goes to zero when the solution is reached.

The second step of the IHB method is the Galerkin procedure. For steady state response, an approximate periodic solution may be assumed as

$$\beta_0 = \sum_{j=0}^{N} \left(a_j \cos\frac{j}{q}\tau_1 + b_j \sin\frac{j}{q}\tau_1 \right),$$

$$\Delta\beta_0 = \sum_{j=0}^{N} \left(\Delta a_j \cos\frac{j}{q}\tau_1 + \Delta b_j \sin\frac{j}{q}\tau_1 \right) \tag{4.4}$$

corresponding to a solution of period 2π—the torque period, where q is the order of subharmonic. Galerkin's method is used with Δa_j and Δb_j as generalized co-ordinates:

$$\int_0^{2q\pi} \{\omega_{00}^2\beta'' + c_1\omega_{00}\beta' + \Delta\beta g_1(\beta_0, \tau_1)\}\delta(\Delta\beta)\,\mathrm{d}\tau_1$$

$$= \int_0^{2q\pi} (R + \Delta\omega S + \Delta\omega_1 E + \Delta\gamma P)\delta(\Delta\beta)\,\mathrm{d}\tau_1. \tag{4.5}$$

An incremental system of $2N$ linear equations in terms of Δa_j and Δb_j is obtained from equation (4.5):

$$C\Delta a = R + \Delta\omega S + \Delta\omega_1 E + \Delta\gamma P, \tag{4.6}$$

where R is the corrective vector, S is the unbalance torque vector due to unit change of $\Delta\omega$, and P is the exciting torque increment vector.

The increments can be solved from the following equation:

$$C\Delta a = R. \tag{4.7}$$

The procedure is repeated until the magnitude of the corrected vector **R** is acceptably small and the solution is obtained.

With the system parameter varied, the system results obtained by the IHB method are compared with the results obtained by numerical integration in the phase planes. There was good agreement between IHB and numerical results calculated by forth order Runge–Kutta method. The phase plane for the non-linear system, equation (2.7), is depicted in Figure 2(a)–2(d) for $d = 0.2$, $d = 0$, $\gamma = 0{,}1$ and $\gamma = 0$ where the symbols "○" and "—" indicate the results obtained by IHB and numerical integration respectively.

5. MELNIKOV'S METHOD

Melnikov [17] developed a global analysis technique on the occurrence of a heteroclinic (or homoclinic) bifurcation. Such a bifurcation is said to have occurred if a heteroclinic (homoclinic) set is either created or destroyed as a parameters is varied. The Melnikov function is a measure of the distance between stable and unstable manifolds when that distance is small. Both the damping and the amplitude of the external torque of the non-linear systems, equation (2.7), are assumed to be small. Assume $d = 0$ and to express equation (2.7) in the dimensionless form, let

$$\omega_n^2 = \frac{mg_0h}{J_{11}}, \quad \tau = \omega_n t$$

and rewrite the equation in the following form:

$$\dot{\beta}_1 = \beta_2,$$

$$\dot{\beta}_2 = \sin\beta_1 + \tfrac{1}{2}\,\bar{Z}(\bar{\beta}_1)\rho^2 + \varepsilon[\gamma\sin\eta\tau\sin\beta_1 - \bar{C}\beta_2], \tag{5.1}$$

where

$$\rho = \frac{\omega_0}{\omega_n}, \quad \eta = \frac{\omega}{n}, \quad \bar{Z}(\beta) = \frac{Z(\beta)}{J_{11}}, \quad \bar{C} = \frac{C}{J_{11}\omega_n}, \quad \tau = \omega_n t.$$

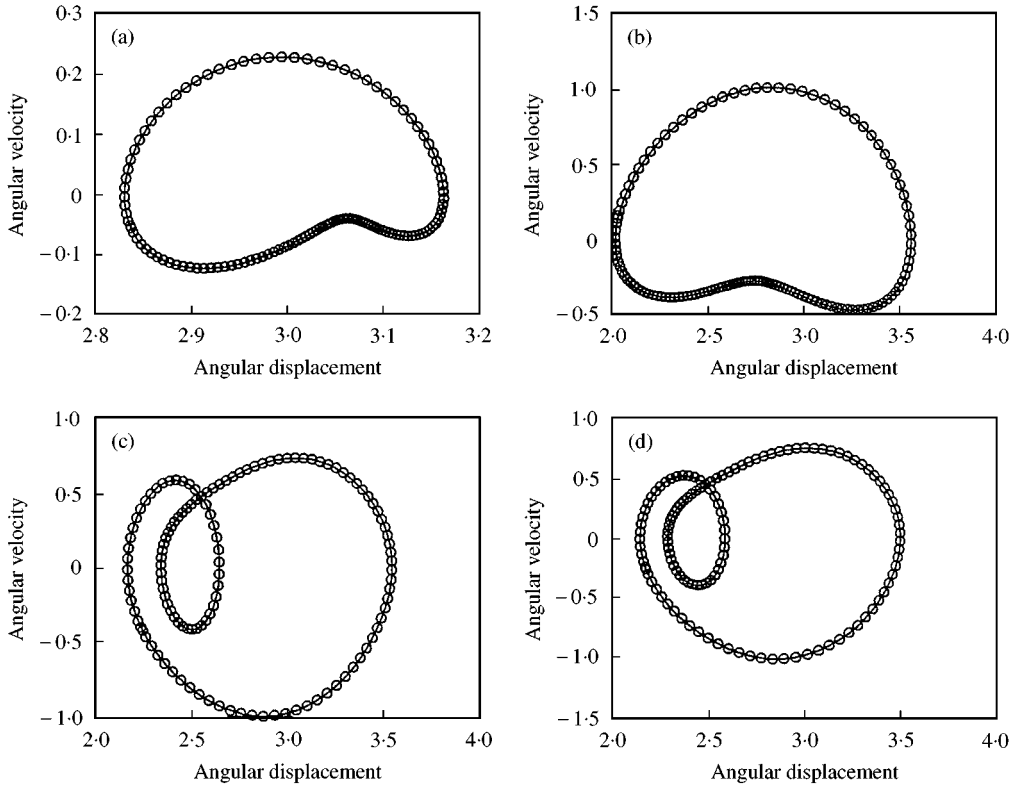

Figure 2. Comparison between the IHB and numerical integration methods: (a) $d = 0{\cdot}2$, (b) $d = 0$, (c) $\gamma = 0{\cdot}1$, (d) $\gamma = 0$.

When $\varepsilon = 0$, the system of equations (5.1) is an unperturbed system and can be reduced to

$$\dot{\beta}_1 = \beta_2,$$

$$\dot{\beta}_2 = \sin\beta_1 + \frac{1}{2}\left[\left(\frac{J_{22} - J_{33}}{J_{11}}\right)\sin 2\beta_1 - 2\,\frac{J_{23}}{J_{11}}\cos 2\beta_1\right]\rho^2. \tag{5.2}$$

The Hamiltonian for the undamped, unforced system is obtained as

$$H = \frac{1}{2}\beta_2^2 + \cos\beta_1 + \frac{1}{4}\rho^2\left[\left(\frac{J_{22} - J_{33}}{J_{11}}\right)\cos 2\beta_1 + 2\,\frac{J_{23}}{J_{11}}\sin 2\beta_1\right]. \tag{5.3}$$

The hyperbolic fixed point p_i^{ε} has stable and unstable manifolds, $W^s(p_i)$ and $W^u(p_i)$. The distance between $W^s(p_i)$ and $W^u(p_i)$ can be measured by the Melnikov functions

$$M_i^{\pm}(\tau_0) = \int_{-\infty}^{\infty} \beta_{2i}^{\pm}(\tau)[-\bar{c}\beta_{2i}^{\pm}(\tau) + \gamma\sin\beta_1\sin\eta(\tau + \tau_0)]\,\mathrm{d}\tau \tag{5.4}$$

for the homoclinic orbits $\Gamma_i^{\pm}$.

Suppose that $M_i^{\pm}(\tau_0)$ has a simple zero, i.e., there exists a point $\tau_0 = \bar{\tau}_0$ such that

$$M_i^{\pm}(\bar{\tau}_0) = 0, \quad \frac{\partial M_i^{\pm}}{\partial\tau_0}(\bar{\tau}_0) \neq 0. \tag{5.5}$$

Then $W^s(p_i^\rho)$ and $W^u(p_i^\rho)$ intersect transversely and there exist transverse homoclinic orbits. Since $\beta_{2i}^{\pm}(\tau)$ is an odd function of τ, equation (5.4) becomes

$$M_i^{\pm}(\tau_0) = -\bar{c}\int_{-\infty}^{\infty}[\beta_{2i}^{\pm}(\tau)]^2\,\mathrm{d}\tau + \gamma\left\{\int_{-\infty}^{\infty}\beta_{2i}^{\pm}(\tau)\sin\beta_1\sin\eta\tau\right\}\mathrm{d}\tau\sin\eta\tau_0$$
$$= -\bar{c}A_i^{\pm} + \gamma B_i^{\pm}\sin\eta\tau_0, \tag{5.6}$$

where

$$A_i^{\pm} = \int_{-\infty}^{\infty}[\beta_{2i}^{\pm}(\tau)]^2\,\mathrm{d}\tau, \quad B_i^{\pm} = \int_{-\infty}^{\infty}\beta_{2i}^{\pm}(\tau)\sin\beta_1\sin\eta\tau\,\mathrm{d}\tau. \tag{5.7}$$

We first consider the case of homoclinic orbits $\Gamma_i^{\pm}$. From equation (5.3) we have

$$\frac{\mathrm{d}\beta_1}{\mathrm{d}\tau} = \mp\sqrt{2H_i - 2\cos\beta_i - \frac{1}{2}\rho^2\left[\left(\frac{J_{22}-J_{33}}{J_{11}}\right)\cos 2\beta_i + 2\frac{J_{23}}{J_{11}}\sin 2\beta_1\right]}, \tag{5.8}$$

on the homoclinic orbits for $\tau > 0$. Hence, if

$$\frac{\gamma}{\bar{c}} > \left|\frac{A_i^{\pm}}{B_i^{\pm}}\right|, \tag{5.9}$$

then $M_i^{\pm}(\tau_0)$ has a simple zero and consequently chaotic dynamics may occur in system (5.1). Criterion (5.9) provides a remarkably good lower bound for the regions of chaos in the $(\eta, \gamma/c)$ space. Comparisons of the Melnikov critical value and the R–K simulation value are shown in Figure 3.

6. PHASE PORTRAITS, POINCARÉ MAP AND POWER SPECTRUM ANALYSIS

The evolution of a set of trajectories emanating from various initial condition is presented in the phase plane. When the solution becomes stable, the asymptotic behaviors of the phase

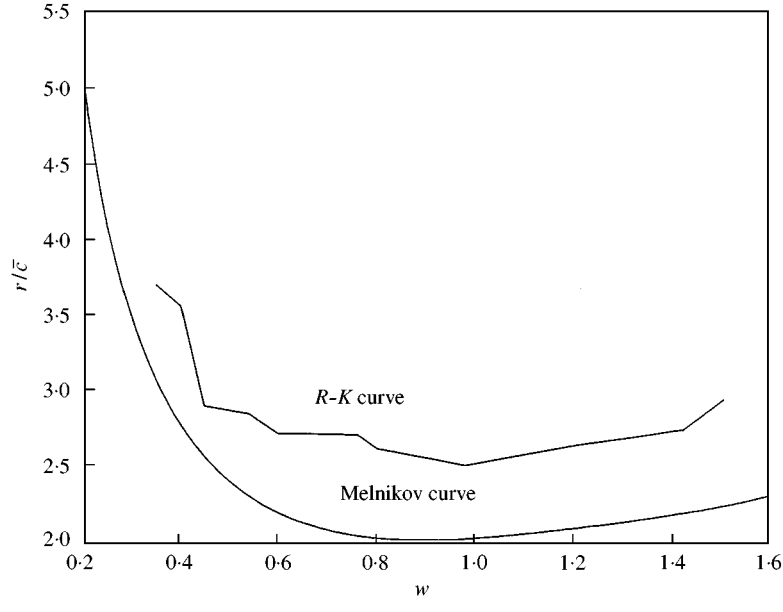

Figure 3. Comparison between the Melnikov and R–K numerical method values

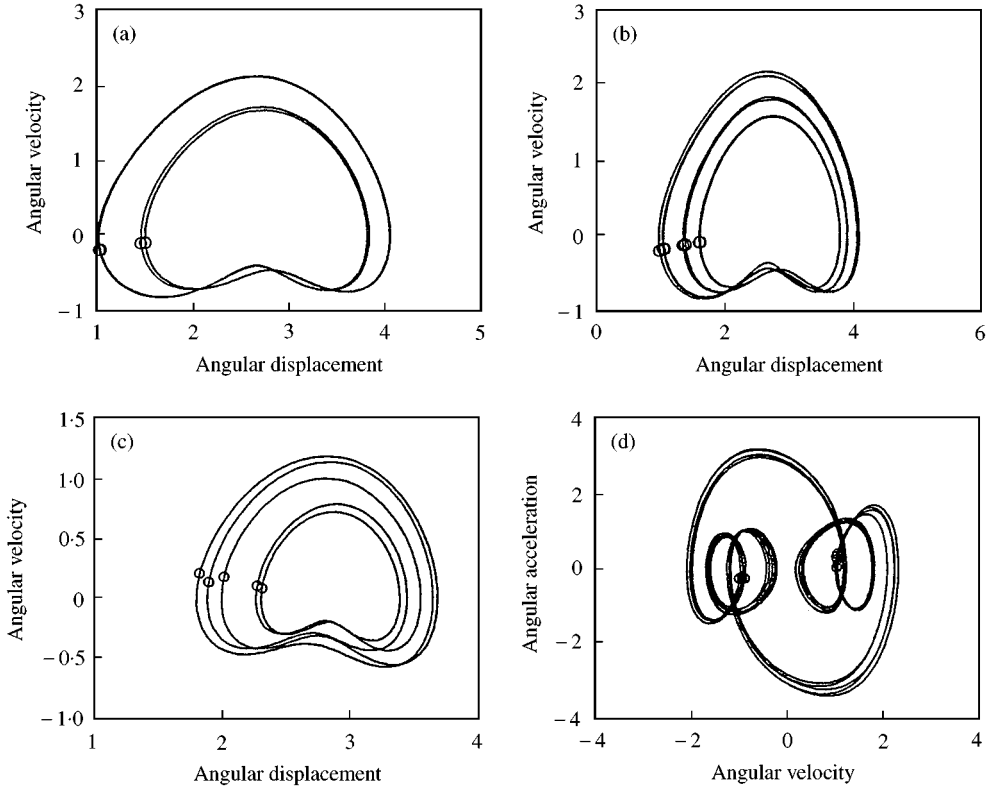

Figure 4. Poincaré maps and phase portraits for different values of γ for $d \neq 0$: (a) $\omega = \omega_s$, $\gamma = 2{\cdot}0$, (b) $\omega = \omega_s$, $\gamma = 2{\cdot}01$, (c) $\omega > \omega_s$, $\gamma = 1{\cdot}5$, (d) $\omega > \omega_s$, $\gamma = 3{\cdot}0$.

trajectories are particularly interesting and the transient behaviors in the system are neglected. The phase portraits of the physical pendulum system, equations (2.7) and (2.8), are plotted in Figure 4(a)–4(d).

The technique introduced by Poincaré deals with the question of the three-dimensional phase space $(\beta, \dot{\beta}, t)$ whenever t is a multiple of $T = 2\pi/\omega$ or $2\pi/\omega_s$. Here T is the period of the external torque. It is constructed by viewing the phase space diagram stroboscopically in such a way that the motion is observed periodically. By using the fourth order Runge–Kutta numerical integration method, the solution of the physical pendulum system obtained by Poincaré maps are shown in Figure 4(a)–4(d), which can be compared with the phase portraits.

Any function $\beta(\tau)$ may be represented as a superposition of different periodic components. The determination of their relative strength is called spectral analysis. Due to the character of the function $\beta(\tau)$, there are two different methods to express $\beta(\tau)$. If it is periodic, the spectrum may be a linear combination of oscillations whose frequencies are integer multiple of a basic frequency. The linear combination is called a Fourier series. If it is not periodic, then the spectrum must be in terms of oscillations with a continuum of frequencies. Such a representation of the spectrum is called Fourier integral of $\beta(\tau)$. The power spectrums of the non-linear dynamical system, equations (2.7) and (2.8) are shown in Figure 5(a)–5(d) respectively. Apparently, the spectrum of the periodic motion only consists of discrete frequencies. The noise-like spectrum is the characteristic of a chaotic dynamical system.

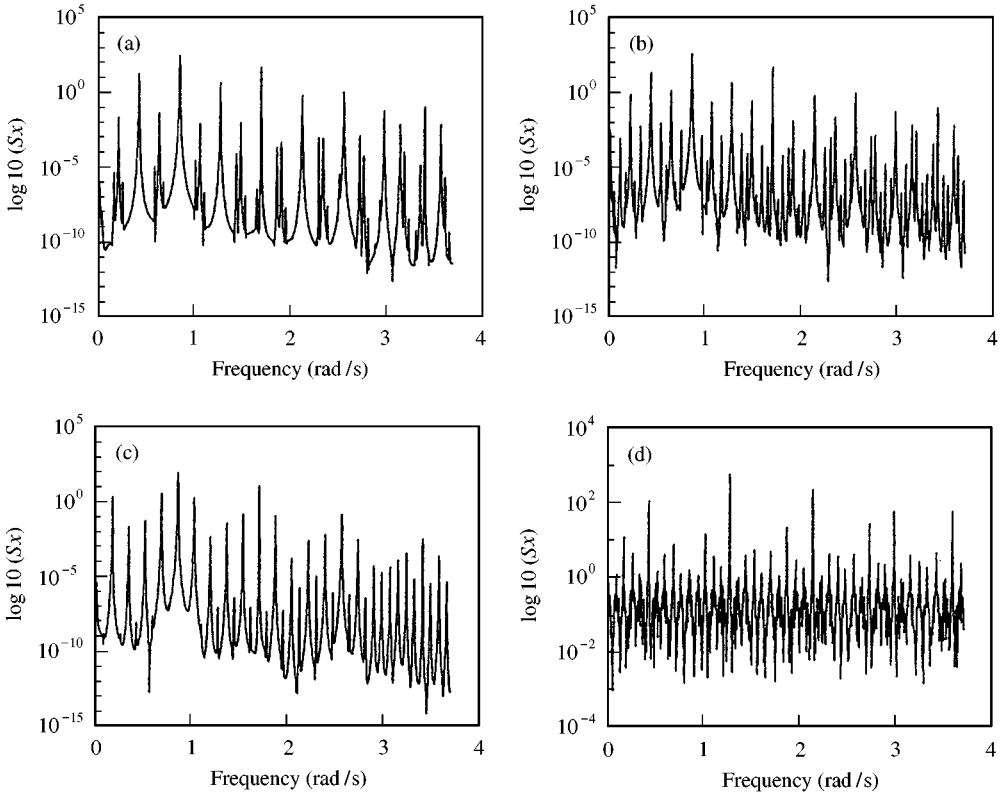

Figure 5. Power spectrum for different values of γ for $d \neq 0$: (a) $\omega = \omega_s, \gamma = 2{\cdot}0$, (b) $\omega = \omega_s, \gamma = 2{\cdot}01$, (c) $\omega > \omega_s$, $\gamma = 1{\cdot}5$, (d) $\omega > \omega_s$, $\gamma = 3{\cdot}0$.

7. BIFURCATION DIAGRAM AND LYAPUNOV EXPONENT

The information about the dynamics of a non-linear system for specific values of the parameters is provided. The dynamics may be viewed more completely over a range of parameter values. As the parameter is changed, the periodic solutions are created or destroyed, or their stability may be changed. The phenomenon of sudden change in the motion as a parameter is varied is called bifurcation, and the parameter value at which it occurs is called bifurcation point.

The bifurcation diagrams of the non-linear system of equations (2.7) and (2.8) are depicted in Figure 6(a) and 6(b). They are calculated by the fourth order Runge–Kutta numerical integration. At each d or γ, the points of Poincaré map in the transient state of motion are discarded.

For Figure 6(a), $\omega = \omega_s$, $d \neq 0$, the pitch fork bifurcations are obvious. But for Figure 6(b), $\omega > \omega_s$, $d \neq 0$ the pattern is changed, the pitch fork bifurcations disappear and the regions of chaos are increased to a large extent.

The Lyapunov exponent may be used to measure the sensitive dependence upon initial conditions. It is an index for chaotic behavior. Different solutions of dynamical system, such as fixed points, periodic motions, quasiperiodic motion, and chaotic motion can be distinguished by it. If two trajectories start close to one another in phase space, they will move exponentially away from each other for short periods of time on the average. Thus, if d_0 is a measure of the initial distance between the two starting points, the distance is

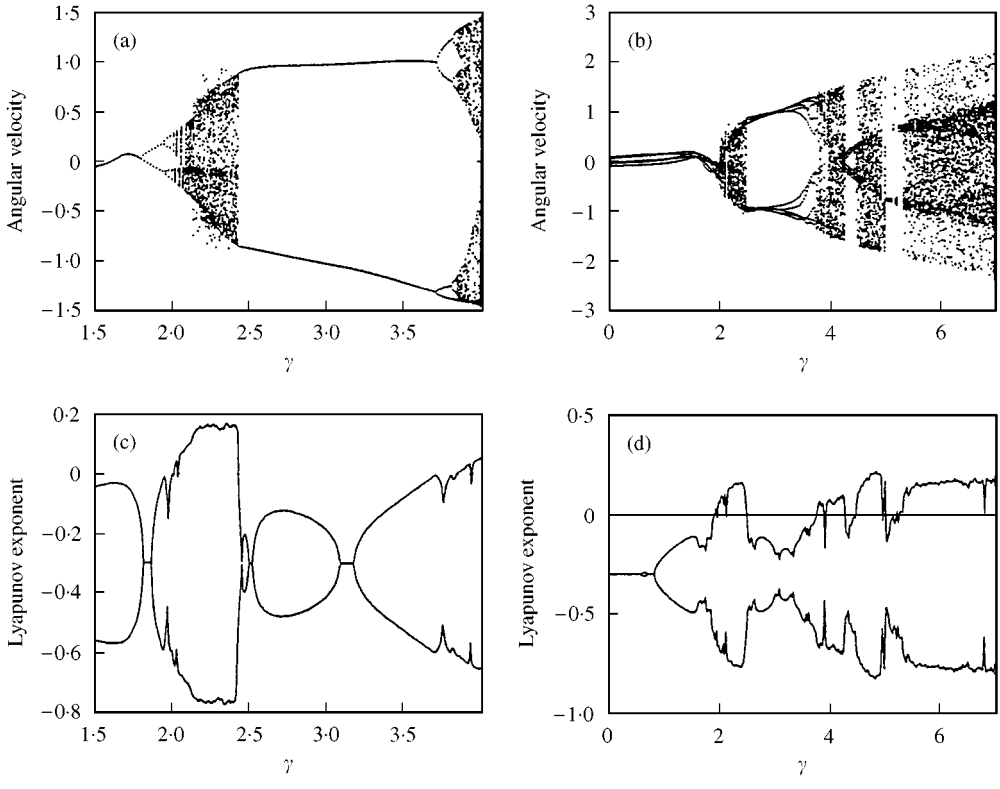

Figure 6. Bifurcation diagram of γ versus angular velocity for: (a) $\omega = \omega_s$, $d \neq 0$, (b) $\omega > \omega_s$, $d \neq 0$ and Lyapunov exponents diagram, (c) $\omega = \omega_s$, $d \neq 0$, (d) $\omega > \omega_s$, $d \neq 0$.

$d(\tau) = d_0 2^{\lambda\tau}$. The symbol λ is called Lyapunov exponent. The divergence of chaotic orbits can only be locally exponential, because if the system is bounded, $d(\tau)$ cannot grow to infinity. A measure of this divergence of orbits is that the exponential growth at many points along a trajectory has to be averaged. The Lyapunov exponent can be expressed as

$$\lambda = \frac{1}{\tau_N - \tau_0} \sum_{k=1}^{N} \log_2 \frac{d(\tau_k)}{d_0(\tau_k - 1)}. \tag{7.1}$$

The signs of the Lyapunov exponents provide a qualitative picture of a system dynamics. The criterion is

$$\lambda > 0 \quad \text{(chaotic)},$$

$$\lambda \leqslant 0 \quad \text{(regular motion)}.$$

The Lyapunov exponents of the non-linear dynamical systems, equations (2.7) and (2.8), are plotted in Figure 6(c) and 6(d).

The bifurcation diagram provides a summary of the essential dynamics and is therefore a useful way to observe non-linear dynamical behavior. To investigate bifurcation further, the phase portraits, Poincaré maps, and power spectra are used. The periodic and chaotic motions could be distinguished by the bifurcation diagram, but the quasiperiodic motion and chaotic motion may be confused. However, they can be distinguished by the Lyapunov exponent method.

8. MODIFIED INTERPOLATED CELL MAPPING METHOD

It is well known that different initial conditions may lead to different attractors when the governing differential equations are non-linear. Hence, how to determine which solution will occur for a given initial conditions is the major task. The attractors and corresponding basins of attraction of this system could be found by using the modified interpolated cell mapping method (MICM) which improved from the interpolated cell mapping method [21]. For a two-dimensional system, the interesting rectangular region of dimensions $n_1 \times n_2$ is divided into $N_1 \times N_2$ cells with size $h_1 \times h_2$. The mapping through MIMC can then be expressed as

$$\bar{P}(x_i + \xi h_1, y_j + \eta h_2) = (1 - \xi)(1 - \eta) P(x_i, y_j) + \xi(1 - \eta) P(x_{i+1}, y_j)$$

$$+ (1 - \xi)\eta P(x_i, y_{j+1}) + \xi\eta P(x_{i+1}, y_{j+1}), \tag{8.1}$$

where

$$0 \leqslant \xi, \quad \eta \leqslant 1.$$

P is the approximate mapping through MICM, $P(x_i, y_j)$ is the actual reference mapping of the point (x_i, y_j) by numerical integration and (x_i, y_j) is the co-ordinate of the center of the (x_i, y_j)th cell.

The wonderful phenomena are called fractal, and the boundary is called fractal basin boundary. In order to observe it, the structure of the fractal basin boundary is enlarged in Figure 7(a)–7(d). Hence, small uncertainties in initial conditions or other system parameters may lead to uncertainties in the consequence of the state of the non-linear system. Thus predictability is not always possible.

9. NON-FEEDBACK CONTROL METHODS

These methods modify the underlying chaotic dynamical system weakly so that stable solutions appear [21], which are arranged as follows

(1) *Controlling of chaos by addition of constant torque.* Interestingly, one can even add just a constant torque to control or quench the chaotic attractor to a desired periodic one in a typical non-linear system. It ensures effective controlling in a very simple way. Examining the effect of the constant torque, the added torque is assumed to be present in equation (2.7). Consider the effect of the constant torque by increasing it from zero upwards; the chaotic behavior is then modified. In Figure 8(a), using constant torque control, chaotic behaviors become P-8T motion for constant torque 0.8.

(2) *Controlling chaos by the second periodic torque*: One can also control system dynamic by the addition of the external second period force in the chaotic state. Equation (2.7) with the second periodic torque $\gamma_2 \sin \Omega\tau$ can be written as

$$\dot{\beta}_1 = \beta_2,$$

$$\dot{\beta} = (\rho\eta d \cos \eta\tau)\bar{b}(\beta_1) + \tfrac{1}{2}\bar{Z}(\beta_1)\dot{\alpha}_1^2 - \bar{C}\dot{\beta}_2$$

$$+ (1 + \gamma \sin \eta\tau) \sin \beta_i + \gamma_2 \sin \Omega\tau. \tag{9.1}$$

When $\gamma_2 \in [1, 5]$ and $\Omega \neq \eta$, the detailed structure of Lyapunov exponent versus γ_2 is shown in Figure 8(b).

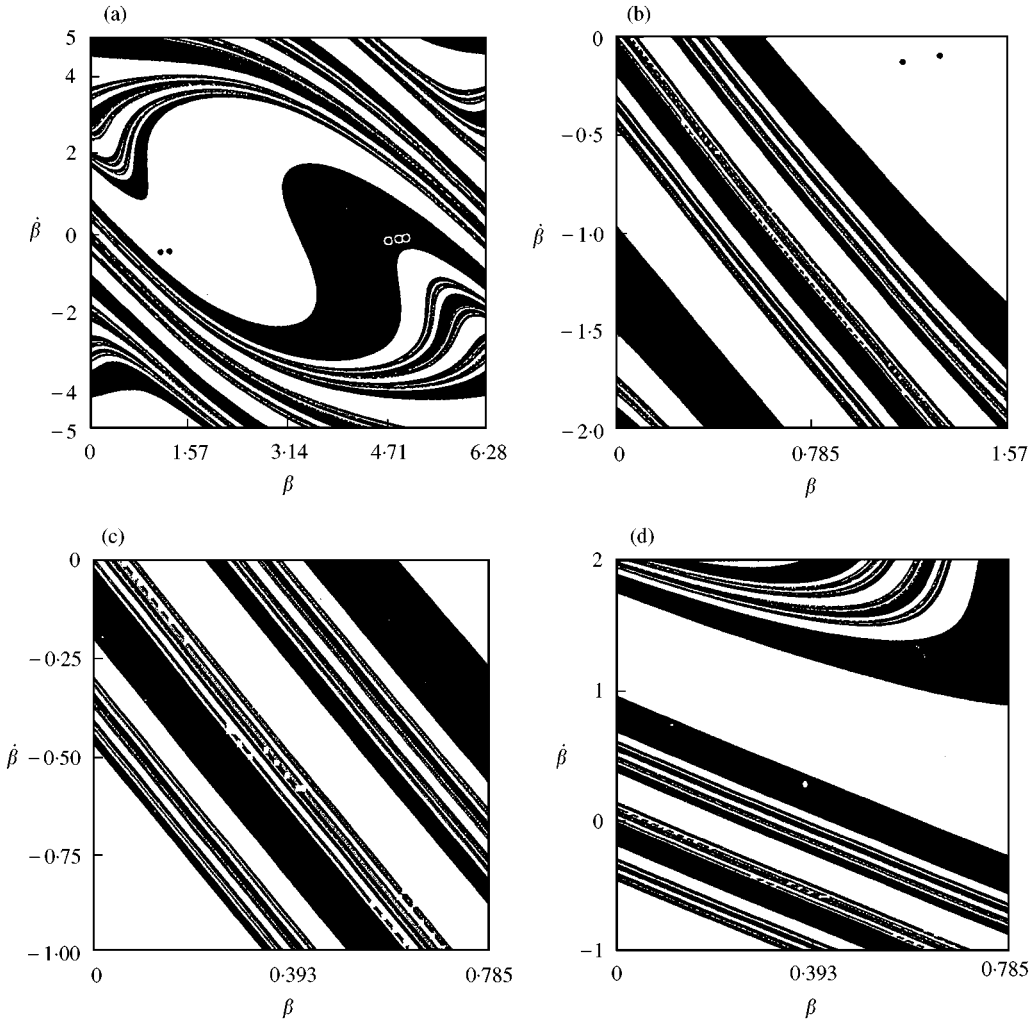

Figure .7 (a) Five attractors coexisting (b)–(d) enlarged fractal diagram of diagram (a).

10. DELAYED FEEDBACK CONTROL

In this section the application of delayed feedback control [22] is introduced. The difference between the delayed output signal $\beta(\tau - \tau_d)$ and the output signal $\beta(\tau)$ is used as a control signal:

$$F(\tau) = K\,[\beta(\tau - \tau_d) - \beta(\tau)], \tag{10.1}$$

where K is the weight of control signal and τ_d is the delay time. Adjusting K and τ_d, we can convert the chaotic motion to periodic motion or even quasi-periodic motion. Figure 8(c), where $K = 0.02$ and $\tau_d = 8\pi$ presents a period-4T periodic motion. Figure 8(d), where $K = 0.04$ presents two quasi-periodic mapping diagrams.

11. ADAPTIVE CONTROL

Adaptive control algorithm was recently suggested [23, 24] for multi-parameter and higher-dimensional non-linear systems. This control mechanism is remarkably effective in

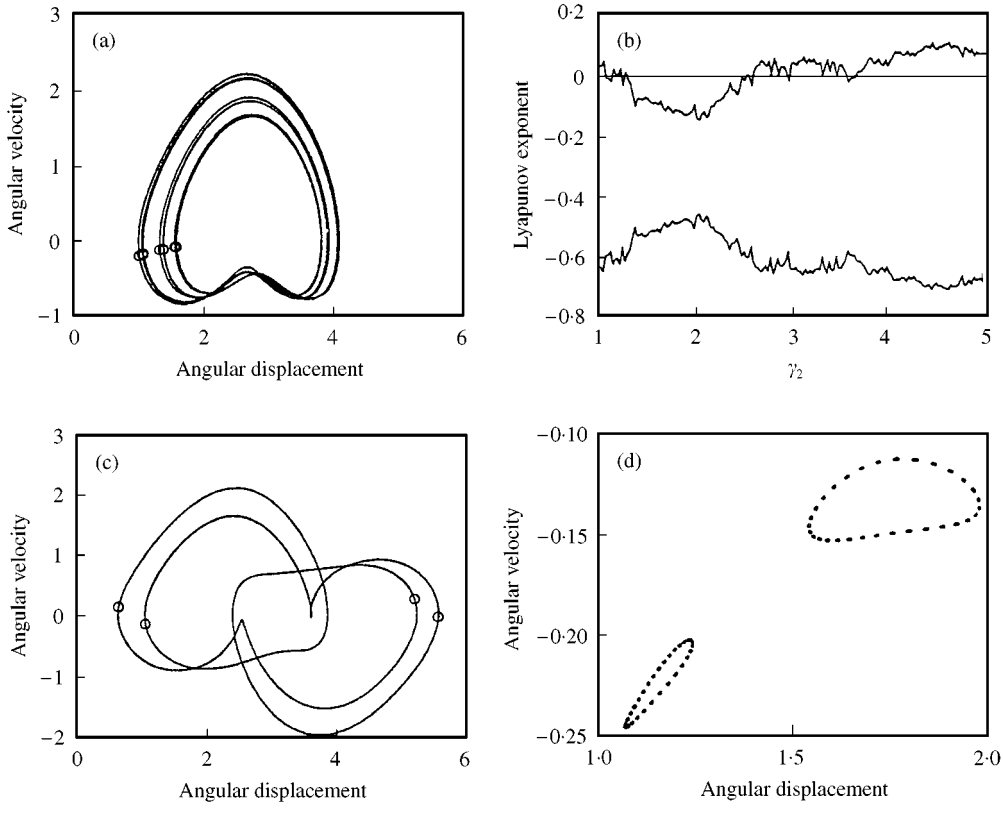

Figure 8. (a) Poincaré maps and phase portraits of non-feedback control of constant torque, (b) Lyapunov exponent for non-feedback control of periodic force, (c)–(d) delayed feedback control.

returning a system to its original dynamics after a sudden perturbation in the system parameter changes the dynamical behavior. This error signal governs the change of the parameter of the system, which readjusts so as to reduce the error to zero. For a general N-dimensional dynamical system

$$\dot{\beta} \equiv \frac{\mathrm{d}\beta}{\mathrm{d}\tau} = F(\beta, \tau, \mu), \tag{11.1}$$

where $\beta \equiv (\beta_1, \beta_2, \ldots, \beta_N)$ are variables and $\mu \equiv (\mu_1, \mu_2, \ldots, \mu_M)$ are parameters, which determine the nature of the dynamics, the prescription for effecting adaptive control is through the additional dynamics

$$\dot{\mu} = \zeta(\beta - \beta_s), \tag{11.2}$$

where β_s is the desired steady state value and ζ indicates the stiffness of control.

This algorithm is remarkably effective and rapid, and is of utility in a large variety of systems, ranging from biological units to control engineering. The efficacy of this idea in application to discrete maps with a signal control parameter has been proved. The recovery time, defined as the time taken to reach the desired state within finite precision after a shock was found to be inversely proportional to the stiffness of control. Adaptive controlling can change chaos motion into periodic motion. The result is shown in Figure 9(a) and 9(b).

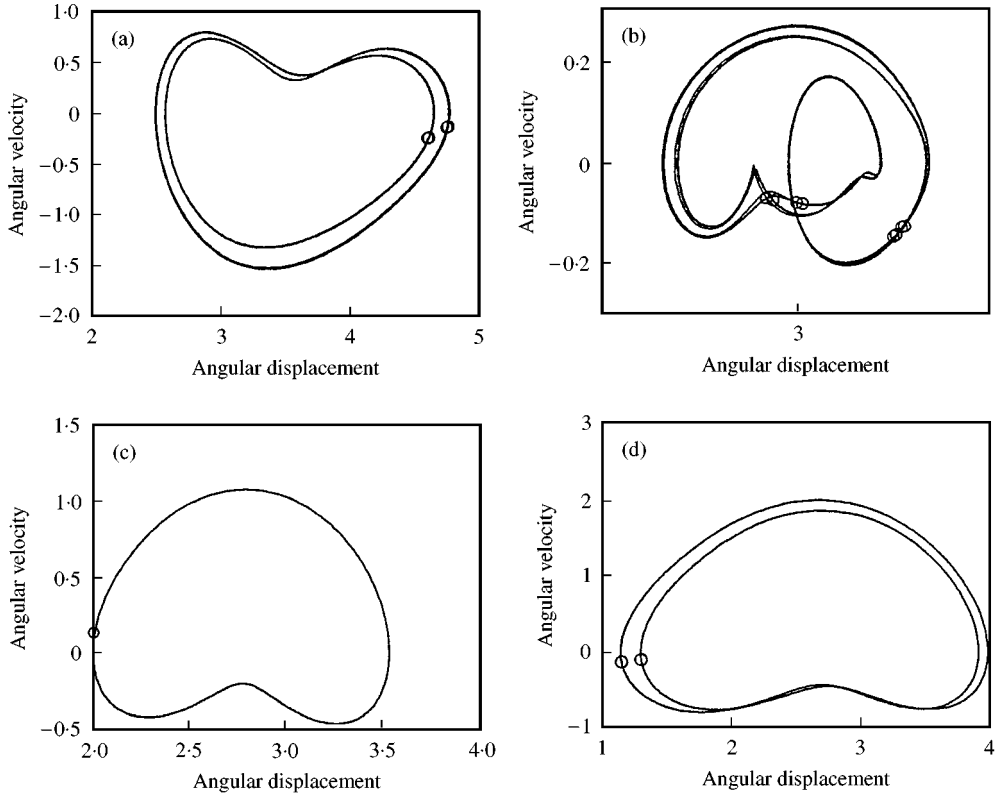

Figure 9. Poincaré maps and phase portraits of (a)–(b) adaptive control, (c)–(d) variable structure control.

12. VARIABLE STRUCTURE CONTROL

In this section, we present the basic principles of the variables structure control theory [25, 26] and their applications in robust control for a class for a class of non-linear oscillators with chaotic attractor. Let us consider the following non-linear oscillators:

$$\dot{\beta}_i = \beta_{i+1}, \quad i = 1, \ldots, n-1,$$
$$\dot{\beta}_n = f(\beta, \tau) + u(\tau) \tag{12.1}$$

where $\beta = [\beta\, \dot{\beta}\, \cdots \beta^{(n-1)}]^{\mathrm{T}}$ is the state vector. The non-linear function $f(\beta, \tau)$ is unknown, but estimated as $\hat{f}(\beta, \tau)$. The estimation error $f(\beta, \tau)$ is assumed to be bounded by some known function $F(\beta, \tau)$

$$|f(\beta, \tau) - \hat{f}(\beta, \tau)| < F(\beta, \tau). \tag{12.2}$$

Assume that the aim of the control system is to track a given desired state vector $\beta_d = [\beta_d\, \dot{\beta}_d\, \cdots\, \beta_d^{(n-1)}]^{\mathrm{T}}$ in spite of model uncertainties. Let $e = \beta_d - \beta$ be the tracking error in the variable β. Furthermore, let us define a time-varying surface $S(\tau)$ in the state-space R^n by the scalar equation

$$s(\beta, \tau) = 0, \tag{12.4}$$

$$s(\beta, \tau) = \left(\frac{\mathrm{d}}{\mathrm{d}t} + \lambda\right)^{n-1} e, \tag{12.5}$$

where λ is a strictly positive constant, will be called the sliding surface. For instance, if $n = 2$,

$$s = \dot{e} + \lambda e. \tag{12.6}$$

It is apparent also that system dynamics while on the sliding surface is determined not from differential equation (12.1) but from equation (12.4) and therefore it is invariant to the parameter variations and structure uncertainty. Initially, however, the state vector β and desired vector β_d do not generally coincide. Let us consider the Lyapunov function candidate

$$V(\beta) = \tfrac{1}{2} s^2. \tag{12.7}$$

The derivative of $V(\beta)$ along the trajectories of the system is given by

$$\dot{V}(\beta) = (\ddot{\beta}_d - f - u + \lambda \dot{e})\, s.$$

The best approximation $\hat{u}$ of a continuous control law that would achieve $\dot{s} = 0$ is then

$$\hat{u} = -\ddot{\beta}_d + \hat{f} - \lambda \dot{e}. \tag{12.8}$$

The $\hat{u}$ can be interpreted as our best estimate of the equivalent control. We add to $\hat{u}$ a discontinuous term across the surface $s = 0$:

$$\hat{u} = \hat{u} - [F(\beta,\ \tau) + \eta]\, \mathrm{sgn}(s), \quad \text{with } \eta > 0. \tag{12.9}$$

Finally, let us consider our dynamic system—a physical pendulum driven by two periodic external forces. The equations considered are

$$\begin{aligned} \dot{\beta}_1 &= \beta_2, \\ \dot{\beta}_2 &= (\rho\eta d \cos\eta\tau)\, \bar{b}(\beta_1) + \tfrac{1}{2}\, \bar{Z}(\beta_1)\, \dot{\alpha}_1^2 - \bar{C}\dot{\beta}_2 \\ &\quad + (1 + \gamma \sin\eta\tau) \sin\beta_1 + u. \end{aligned} \tag{12.10}$$

The result is shown in Figure 9(c) and 9(d).

13. CONCLUSION

The dynamical system of the physical pendulum with damping subjected to two exciting torques exhibits a rich variety of non-linear behaviors as unequivocal parameters are varied. Due to the effect of non-linearity, regular or chaotic motions may appear. In this paper, analytical, computational methods and controlling of chaos have been employed to study the dynamical behaviors of the non-linear system.

The stability conditions for the physical pendulum system have been found by using the Lyapunov direct method. The IHB method uses fast-Fourier transform (FFT) and must be used by trying various initial conditions. Further, the existence of chaotic motion has been identified by Melnikov's method.

The computational analyses have been performed. The bifurcation of the parameter-dependent system has been studied numerically. The time evolutions of non-linear dynamical system response have been described using the phase portraits via the Poincaré map technique. The occurrence and nature of chaotic attractors have been verified by evaluating Lyapunov expenont and power spectra. Finally, global analysis of the basin boundary and fractal structure have been observed by the MICM method.

We have demonstrated that a simple control strategy can be effectively used to suppress chaos in a non-linear dynamical system. It is our hope that similar control strategies can be successfully implemented for more situations. By using a number of analytical or

computational methods, the non-linear behaviors of the physical pendulum like the different types of periodic solutions, the effects on the solutions caused by different parameters and initial condition, the stability analysis of solutions have been studied. In spite of the fact that these methods are different, the results obtained match each

REFERENCES

1. N. N. BOLOTNIK 1994 *Journal of Applied Mechanics* **58**, 841–848. Inertial motion of an absolutely rigid body on two-degree-of-freedom joint.
2. A. P. MARKEYEV 1990 *Theoretical Mechanics*, Moscow: Nauka.
3. R. A. STRUBLE 1963 *Journal of Applied Mechanics* **44**, 301–303. On the subharmonic oscillations on a pendulum.
4. T. V. SKALAK and M. I. YARYMOVYCH 1960 *Journal of Applied Mechanics* **44**, 159–164. Subharmonic oscillations on a pendulum.
5. C. S. HSU 1975 *Journal of Applied Mechanics* **42**, 176–182. Limit cycle oscillations of parameter excited secondorder nonlinear system.
6. M. J. CLIFFORD and S. R. BISHPO 1993 *Physics Letters A* **184**, 57–63. Generic features escape from a potential well under parameter excitation.
7. E. G. GWINN and R. M. WESTERVELT 1986 *Physica D* **23**, 369–401. Horseshoes in the driven damped pendulum.
8. E. G. GWINN and R. M. WESTERVELT 1986 *Physical Review A* **33**, 4143–4155. Fractal basin boundary and intermittency in the driven damped pendulum.
9. M. VIDYASAGAR 1993 *Nonlinear Systems Analysis*. London: Prentice-Hall.
10. H. K. KHALIL 1996 *Nonlinear Systems*, second edition. Englewood Cliffs, NJ: Prentice-Hall.
11. M. SKOWRONSKI 1990 *Nonlinear Liapunov Dynamics*. New York: World Scientific Publishing Co.
12. W. WONG, W. S. ZHANG and S. L. LAU 1991 *Journal of Sound and Vibration* **149**, 91. Periodic forced vibration of unsymmetrical piecewise-linear systems by incremental harmonic balance method.
13. Y. K. CHEUNG and S. H. CHEN 1990 *Journal of Sound and Vibration* **140**, 273–286. Application of the incremental harmonic balance method to cubic non-linearity systems.
14. P. G. PIERRE and E. H. DOWELL 1986 *Journal of Applied Mechanics* **52**, 693–697. A study of dynamic instability of plates by an extended incremental harmonic balance method.
15. L. LAU and W. S. ZHANG 1992 *Journal of Applied Mechanics* **59**, 153–160. Nonlinear vibration of piecewise-linear systems by incremental harmonic balance method.
16. P. G. PIERRE, A. A. FERRI and E. H. DOWELL 1985 *Journal of Applied Mechanics* **52**, 958–964. Multi-harmonic analysis of dry friction damped systems using an incremental harmonic balance method.
17. K. YAGASAKI 1994 *Nonlinear Dynamics* **6**, 125–142. Chaos in a pendulum with feedback control.
18. A. WOLF, J. B. SWIFT, H. L. SWINNEY and J. A. VASTANO 1985 *Physica D* **16**, 285–317. Determining Lyapunov exponent from a time series.
19. Z. M. GE and S. C. LEE 1997 *Journal of Sound and Vibration* **192**, 189–206. A modified interpolated cell mapping method.
20. H. TONGUE and K. GU 1998 *Journal of Applied Mechanics* **55**, 461–466. Interpolated cell mapping of dynamical systems.
21. S. RAJASEKAR and M. LAKSHMANAN 1993 *Physica D* **67**, 282–300. Algorithms for controlling chatic motion: application for the BVP oscillator.
22. K. PYRAGAS and A. TAMAŠEVICIUS 1993 *Physics Letters A* **180**, 99–102. Experimental control of chaos by delayed self-controlling feedback.
23. B. A. HUBERMAN and E. LUMER 1990 *IEEE Transactions of Circuits Systems* **37**, 547–550. Dynamics of adaptive system.
24. S. SINHA, R. RAMASWAMY and J. S. RAO 1991 *Physica D* **43**, 118–128. Adaptive control in nonlinear dynamics.
25. S. V. DRAKUNOV and V. I. UTKIN 1992 *International Journal of Control* **55**, 1029–1037. Sliding mode control in dynamic system.
26. J.-J. E. SLOTINE and W. LI 1991 *Applied Nonlinear Control*. Englewood Cliffs, NJ: Prentice-Hall.